Journal of Cancer Research and Clinical Oncology (2023) 149:6501–6511
https://doi.org/10.1007/s00432-023-04604-6

RESEARCH

Antitumor activity of triazine mimic antibiotics for DNA-binding implications (impressive activity in vitro against a variety of tumor types in the NCI-60 screen): NSC 710607 to fight HCT-116 human colon carcinoma cell lines in vivo using the hollow fiber assay and xenograft mouse models

Jaroslaw Spychala[1]

Received: 5 December 2022 / Accepted: 25 January 2023 / Published online: 13 February 2023

Abstract

Purpose Successful clinical applications of DNA-directed selective cytotoxic agents disrupt the vital replication/transcription processes and ultimately lead to cancer cell death. This study aimed to examine the growth screen of two lead triazine compounds in a number of cell lines and xenografts and to develop anticancer agents with noncovalent binding affinity bringing fewer side effects.

Methods The NCI initial hollow fiber test was performed using an established procedure. The cytostatic and cytocidal capacities of the test compounds were assessed by evaluating cytotoxicity by simply performing a standard cellular viability assay. The nude mouse human tumor xenograft system was used as an in vivo model.

Results More sensitive drug with sub-micromolar activity met the interdisciplinary criteria for testing and was referred to evaluations in subcutaneous colorectal carcinoma HCT-116 human tumor xenografted into nude mice. Principal findings of the study: total cytostasis, almost nontoxic schedules, specific working hypotheses, strong rationale for the potential use, and important general implications (relevance to human biology). NSC 710607 displayed in vivo better than Cisplatin and 5-fluorouracil abilities to significantly decrease tumor growth.

Conclusion Cell proliferation can be reduced or stopped in vivo in view of the xenograft results. The mimic molecule behaves as DNA-binding antitumor antibiotics with great potential as general anticancer agents and deserves further trials. NSC 710607 represents the result of a design strategy with outstanding potential. This study also identifies the prognostic significance and is likely to translate to other species or systems.

Keywords HCT-116 colorectal carcinoma · Hollow fiber assay · Large-scale NCI-60 · Mechanisms of cancer · Mouse xenografts · MV-3 human melanoma

Introduction

The minor and major grooves are powerful acceptors for specific associated enzymes in the processing and expression of genomic DNA, and therefore small mimic molecules (reversible and irreversible agents) are capable of interacting with the appropriate recognition sequences (Spychala 2009, 2008, 2006; Boykin et al. 1995; McConnaughie et al. 1994; Spychala et al 1994). Also poisoning of topoisomerases may contribute to the cytotoxic effect of the drug (Mastrangelo et al 2022; McClendon et al. 2007; Coleman et al. 2002; Burden et al. 1998).

Drugs that bind to the minor groove of cell-free nucleic acids (sequence DNA-selective agents) can be expected to have the potential to disrupt gene expression, thereby contributing to antitumor effects. Numerous cellular enzymatic mechanisms can directly repair damaged DNA, or allow tolerance of DNA lesions. The role of AT-rich DNA recognition sequences appears to be extremely important in gene regulatory processes—an ideal target for small molecules recognizing these sequences with high affinity and

✉ Jaroslaw Spychala
jjspychala@wp.pl; jjspychala@interia.pl

[1] Poznan, Poland

selectivity (Ogbonna et al. 2022; Nelson et al. 2007; Li et al. 2007; Hendry et al 2007; Wemmer and Dervan 1997).

Different binding affinity or stability emphasizes the importance of diamidines to the anticancer activity. Prediction of their activity in humans from in vitro data could substantially reduce the number of failures. New selective therapeutic agents are needed for the treatment of colorectal carcinoma cancer, one of the leading causes of malignant mortality worldwide (Xie et al. 2022; Syriopoulou et al. 2019; Van Cutsem et al. 2015; Kraus and Arber 2009). One approach to prediction of the expected active doses in humans or animals from the first in vitro studies has been presented for compounds having unique structures (Spychala 2009).

The targeting of mutated cancer genes by specific drugs has been a widely unexplored possibility in cancer chemotherapy. Parameters, such as dimensions, hydrogen bonding capabilities, hydrophobicity, electrostatics, hydration state, as well as structure flexibility, decide about the best anticancer selectivity. All of these structural and electronic factors contribute to the recognition of mutated sequences by small molecules.

While tremendous efforts in genetics research have been focused on naturally occurring DNA sequence variations and functional characterization of the mutated genes, the structural insights into DNA mutation patterns are still unexplored in depth (Gu et al. 2022; Zhang et al. 2022; Torkamani et al. 2009). In that way, small modifications of typical DNA binders are the major contributors favoring the mutation binding mode of new affinity analogs (size selectivity). The putative complexes are believed to be the trigger for apoptosis.

The anticancer screening profiles and diverse biological properties described in literature have been of particular interest for studying selectivity and mechanism of action as well as for the access to some predictive data on the effects on normal cells (treatment selectivity). The results collectively confirm that both drugs in Fig. 1 can induce DNA damage. In the present work, a positive correlation of the in vitro response parameters with the in vivo evaluation in two models is described.

Methods

Cell culture, screening systems, and cytotoxicity

Triazine diamidines NSC 710607 and NSC 710608 are the original author samples (Spychala 2006, 1999). The Sulforhodamine B (SRB) assay measures total protein content

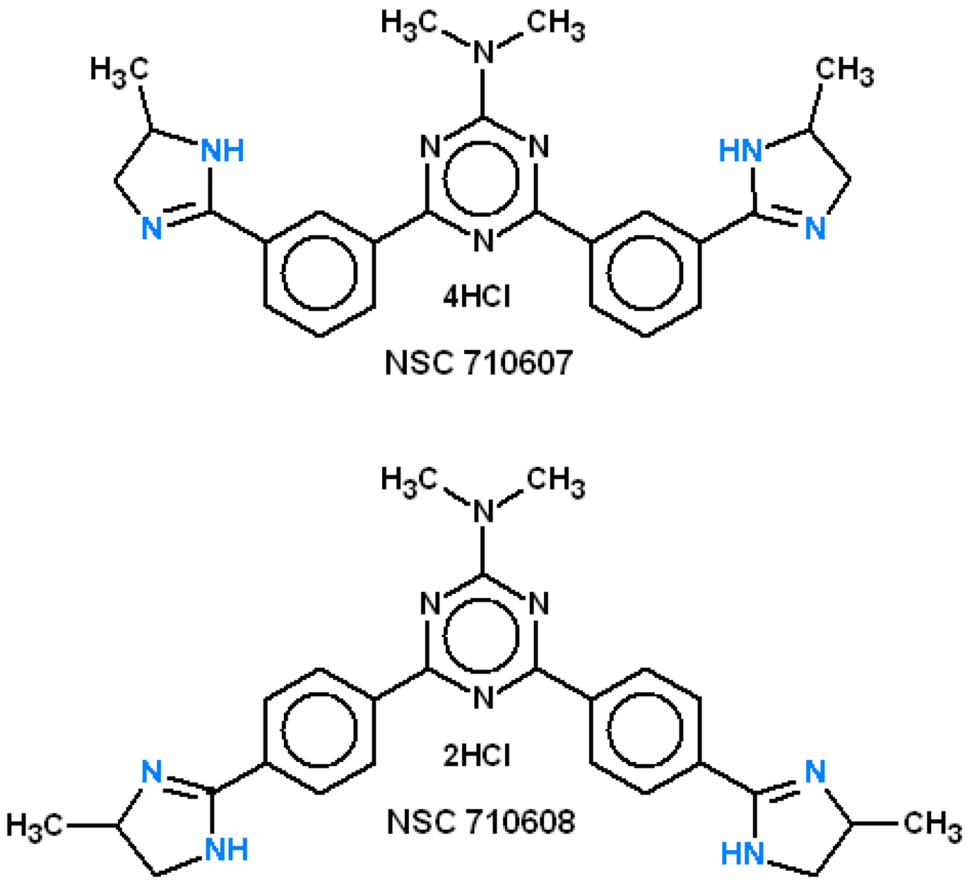

Fig. 1 Chemical structures of two triazine bisimidazolines selected for the in vivo hollow fiber screen as leads from the NCI-60 large-scale screen. A strategy for predicting the chemo-sensitivity of human cancers and its application to drug discovery shows great promise

of the surviving cells at 48 h of drug exposure (Shoemaker 2006). Percentage Growth (PG) was calculated by comparing the growth in drug-free control cultures. Meangraph Midpoint (MG_MID) at the parameter GI_{50}: averaged value of the concentrations needed for 50% growth inhibition over all cell lines in the NCI-60 screen. The highest test dose was 100 µM; the lowest test dose was 0.01 µM. Principal response parameters: range (R), delta (Δ), GI_{50}, TGI, and LC_{50} were previously defined (Spychala 2009).

Percentage Growth (PG) was calculated by comparing the growth in drug-free control cultures according to one or the other of the following two expressions: if (Mean OD_{test} – Mean OD_{tzero}) ≥ 0, then PG = 100 × (Mean OD_{test} – Mean OD_{tzero})/(Mean OD_{ctrl} – Mean OD_{tzero}); if (Mean OD_{test} – Mean OD_{tzero}) < 0, then PG = 100 × (Mean OD_{test} – Mean OD_{tzero})/Mean OD_{tzero}, where Mean OD_{tzero} = the average of optical density measurements SRB-derived color just before exposure of cells to the test compound, Mean OD_{test} = the average of optical density measurements SRB-derived color after 48 h exposure of cells to the test compound, Mean OD_{ctrl} = the average of optical density measurements SRB-derived color after 48 h with no exposure of cells to the test compound.

The NCI standard hollow fiber assay mimicked xenograft implantation (Plowman et al. 1997). The assay involved the implantation of 1 mm I.D. polyvinylidene fluoride 'hollow fibers', with a molecular weight exclusion of 500,000 Da, containing various tumor cells into immunologically compromised mice to provide an assay that mimicked xenograft implantation. The fibers heat-sealed at 2 cm intervals were filled with cells (placed into tissue culture medium and flushed) and incubated prior to implantation.

A total of three different tumor lines were prepared for each experiment so that each mouse received three intraperitoneal and three subcutaneous implants. The cell lines were cultivated in RPMI-1640 containing 10% FBS (fetal bovine serum) and 2 mM glutamine. On the day preceding the hollow fiber preparation, it was given the cells a supplementation of fresh medium to maintain log phase growth. They were harvested by standard trypsinization technique, collected by centrifugation, and re-suspended in the conditioned medium.

Cells of the HCT-116 human colon cancer line were transplanted subcutaneously to female NCr *nu/nu* mice (10^7 cells/mouse, day 0). Nude mouse models were maintained under pathogen-free conditions in the animal facility of the Max-Delbrueck-Center for Molecular Medicine, Berlin, Germany (McIntyre et al. 2015; Dowling et al. 2008), following institutional guidelines and with approval from the responsible authorities. The mice were held in laminar flow shelves in germ-poor conditions at 25 °C, 50% relative humidity, and a 12 h light–dark rhythm. They were given ad libitum access to autoclaved food and bedding, and acidified drinking water.

When the tumors had reached a size of about 4–5 mm diameter, several mice groups were treated intravenously with NSC 710607. Tumor diameters were measured on the indicated days in two perpendicular dimensions with a caliper-like instrument. Treated to control values (T/C) as percentages were calculated from the mean tumor volumes of each group, according to the following empirical equation: $V = (\text{length} \times \text{width}^2)/2$. The optimum value was used for the evaluation of sensitivity or resistance.

Results

The NCI-60 large-scale in vitro results

Differences in apparent selectivity patterns were noted (Fig. 2). There is selectivity for tumor cells versus normal cells in culture. Comparison between differential activity patterns is advantageous for the reason of relative drug sensitivity in cell cultures. The particular colon cell line curves of NSC 710607 and NSC 710608 are grouped by subpanel in Fig. 3. The experimental data of NSC 710607 and NSC 710608 collected against each cell line in the NCI-60 screen are presented and response parameters expressed as the $-\log_{10}$ (Tables 1 and 2). Dose–response curves were made by plotting PGs against the log of the corresponding concentration for every cell line (five-log dose range at ten-fold dilutions).

Cytostatic and cytotoxic effects of NSC 710607

Values in parentheses in Table 3, for the NCI in vitro parameters, are with the exclusion of three untypical deviated cell lines (the least sensitive ones in either case: HCT-15, CAKI-1, NCI/ADR-RES). They are calculated for the close enough dose–response growth characteristics. Significant increases in the Δ (logarithm of difference between the appropriate MG-MID and the log GI_{50} for the most sensitive cell line emphasized in Fig. 2) and Δ_1 (HCT-116) parameters of NSC 710607 give evidence of better selectivity.

The percentage growths were − 29% and − 91% at 10^{-5} and 10^{-4} M, respectively, for the most active colon cell line HCT-116 treated with NSC 710607 (Fig. 3). The appropriate data for NSC 710608 were − 99% at 10^{-4} M and − 37% at 10^{-5} M. Considerable dissimilarity at 10^{-6} M dose level is seen: 33% for NSC 710607 and 71% for NSC 710608. Cytostatic (cytotoxic) effects for the HCT-116 were reached at 3.45×10^{-6} M (2.21×10^{-5} M) for NSC 710607 and 4.52×10^{-6} M (1.60×10^{-5} M) for NSC 710608, respectively.

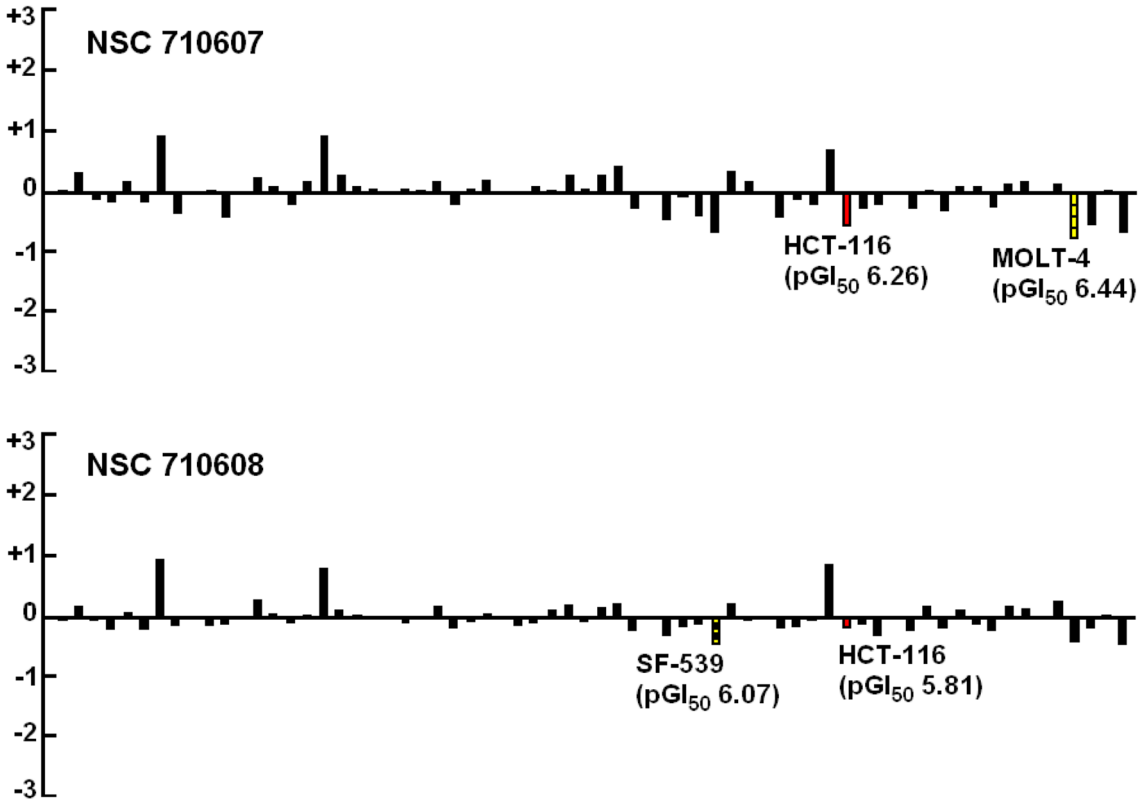

Fig. 2 Visual scanning of pGI_{50} data from the large-scale in vitro cell line screen for two potential diamidine drugs. Bars extending in to the top (positive values) correspondingly imply the sensitivity less than the mean and these activities usually are of little consideration, drug concentrations are strongly suspected of having toxicity versus normal cells

Cytostatic and cytotoxic effects of NSC 710608

While compounds NSC 710607 and NSC 710608 share important similarities in the average GI_{50}, TGI, and LC_{50} activities, the NCI-60 activity profile of NSC 710607 displays a superior proliferation-suppressive capability in colon cells (Fig. 3). The HCT-116 cells, with a GI_{50} of 1.55 µM, were found to be 3 times less sensitive toward the drug NSC 710608 than NSC 710607 with the GI_{50} value observed in the sub-micromolar concentration range at 0.55 µM (Spychala 2008).

Large-scale NCI-60 screen was performed to estimate reproducibility of the in vitro results. Both cytostatic and cytotoxic outcomes were confirmed from the large-scale NCI anticancer drug screen by comparison with the appropriate standard screen response parameters: NSC 710607 (pMG_MID GI_{50} 5.78, pMG_MID TGI 5.22, pMG_MID LC_{50} 4.62) and NSC 710608 (pMG_MID GI_{50} 5.68, pMG_MID TGI 5.17, pMG_MID LC_{50} 4.63). The two agents resemble each other in the number of cancer cells showing the cytostatic and cytotoxic effects.

Preliminary in vivo hollow fiber-based screening

Table 3 presents in vivo data for NSC 710607 and NSC 710608, along with their evaluation in the NCI-60 cell screen. Each compound was tested against a standard panel of 12 human tumor cell lines including NCI-H23, NCI-H522, MDA-MB-231, MDA-MB-435, SW-620, COLO 205, LOX IMVI, UACC-62, OVCAR-3, OVCAR-5, U251, and SF-295. The effects of compounds on reduction of viable cancer cell mass compared to those of controls were determined.

NSC 710607 has been evaluated as an anticancer agent in subcutaneous human tumor xenograft assays on the basis of several hollow fiber assay criteria: a reduction in net cell growth of 50% or greater in 10 by 48 possible test combinations, a reduction in net cell growth of 50% or greater in a minimum of 4 by 24 distant site combinations, and/or cell kill of one or more cell lines in either implant site (reduction in the viable cell mass below the level present at the start of the experiment).

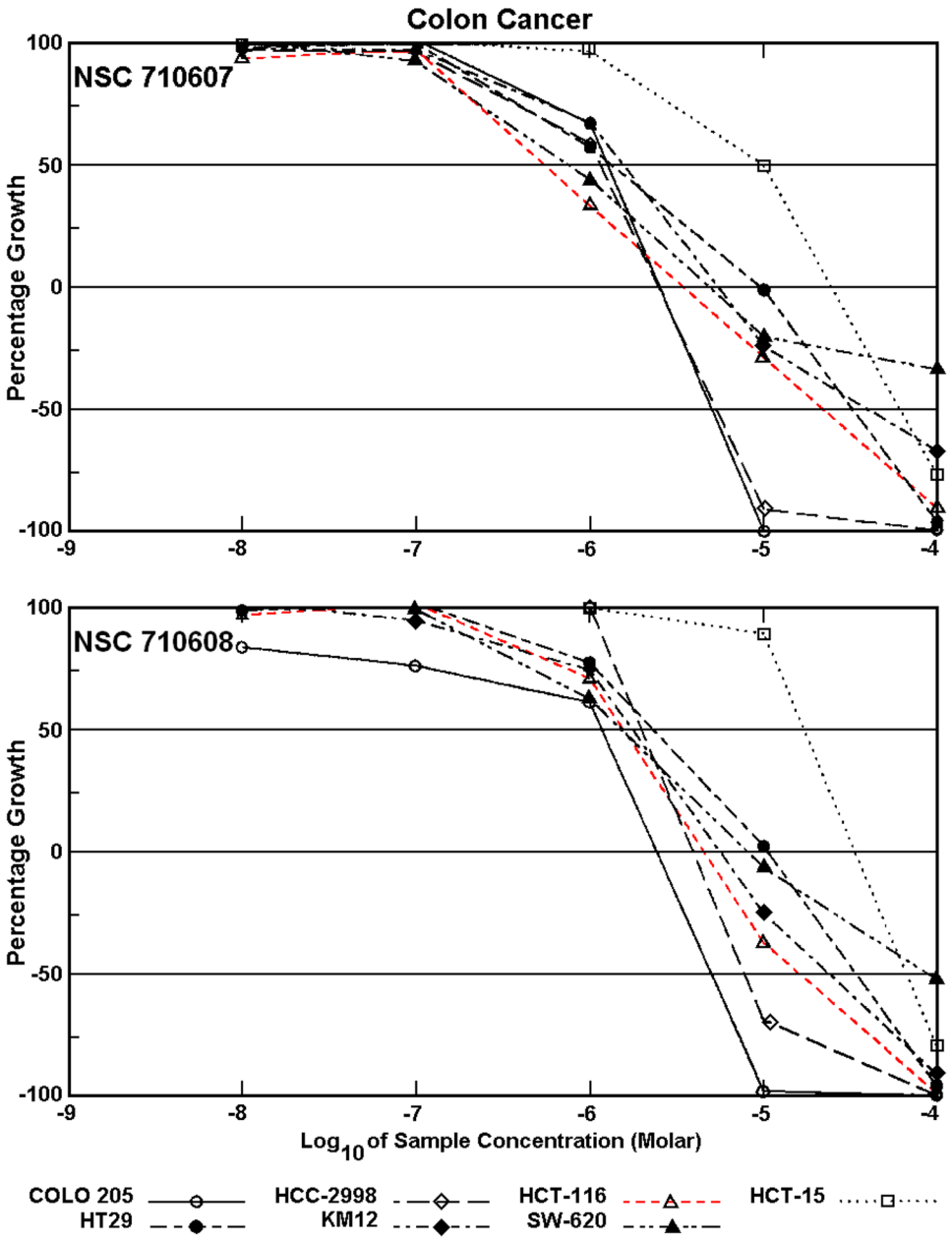

Fig. 3 Representation of all colon dose–response curves in the large-scale NCI-60 cell line screen. Mechanistic insight into two triazine compounds is provided on the basis of the hypothesis that comparable anticancer characteristics signify similar mechanisms of action

A point system adopted has been applied. In a general way, a score of two was assigned each time the compound produced a 50% or greater reduction in viable cell mass compared to vehicle controls. The score for each compound was summed up for the intraperitoneal (IP) fibers and the separate subcutaneous (SC) fibers to provide the total score for each derivative.

Compounds with a combined IP + SC score 20, an SC score 8 or a net cell kill of one or more cell lines are referred for further studies. These criteria were statistically validated by comparing the activity outcomes of more than 80 randomly selected compounds in the hollow fiber assay and xenograft testing. Using this scoring system, the in vivo antitumor analysis in Table 3 confirmed the better differential activity pattern. It follows that NSC 710607 warrants further testing in additional animal models.

Human colon cancer HCT-116 xenografted in nude mice

The mice were randomly divided into four treatment groups: (A) vehicle control, Saline plus Tween® 80—nonionic detergent and emulsifier, (B) 20 mg/kg, (C) 40 mg/kg, and (D) 50 mg/kg of NSC 710607 (Table 4). Tumors were measured six times during a 3-week treatment period. All mice

Table 1 Cytostatic and cytotoxic effects of NSC 710607.

4,6-Bis[3-(4,5-dihydro-4-methyl-1*H*-imidazol-2-yl)phenyl]-2-dimethylamino-1,3,5-triazine tetrahydrochloride	
Panel	Cell lines (cytotoxicity: pTGI > 4.00)
Leukemia	CCRF-CEM (5.57), HL-60(TB) (5.32), K-562 (5.56), MOLT-4 (5.44), RPMI-8226 (5.05)
Non-small cell lung cancer	A549/ATCC (4.96), EKVX (4.88), HOP-62 (5.20), HOP-92 (4.75), NCI-H23 (4.97), NCI-H322M (5.37), NCI-H460 (5.32), NCI-H522 (5.55)
Colon cancer	COLO 205 (5.60), HCC-2998 (5.61), HCT-116 (5.46), HCT-15 (4.61), HT29 (5.02), KM12 (5.26), SW-620 (5.31)
CNS cancer	SF-268 (4.86), SF-295 (4.78), SF-539 (5.78), SNB-19 (5.37), SNB-75 (5.44), U251 (5.68)
Melanoma	LOX IMVI (5.59), MALME-3 M (4.75), M14 (4.87), SK-MEL-2 (5.32), SK-MEL-28 (4.77), SK-MEL-5 (5.29), UACC-257 (5.14), UACC-62 (5.40)
Ovarian cancer	IGROV1 (4.81), OVCAR-3 (5.25), OVCAR-4 (5.47), OVCAR-5 (4.89), OVCAR-8 (4.90), SK-OV-3 (5.23)
Renal cancer	786–0 (4.98), A498 (5.15), ACHN (4.94), CAKI-1 (4.52), RXF 393 (5.02), SN12C (5.35), TK-10 (5.16), UO-31 (4.95)
Prostate cancer	PC-3 (5.46), DU-145 (5.19)
Breast cancer	MCF7 (5.47), NCI/ADR-RES (4.45), MDA-MB-231/ATCC (5.43), HS 578 T (4.73), MDA-MB-435 (5.54), MDA-N (5.37), BT-549 (4.79), T-47D (4.92)
Panel	Cell lines (cytotoxicity: $pLC_{50} > 4.00$)
Leukemia	CCRF-CEM (< 4.00), HL-60(TB) (4.63), K-562 (< 4.00), MOLT-4 (4.05), RPMI-8226 (< 4.00)
Non-small cell lung cancer	A549/ATCC (4.23), EKVX (4.29), HOP-62 (4.37), HOP-92 (< 4.00), NCI-H23 (4.33), NCI-H322M (4.71), NCI-H460 (4.88), NCI-H522 (5.12)
Colon cancer	COLO 205 (5.30), HCC-2998 (5.27), HCT-116 (4.66), HCT-15 (4.22), HT29 (4.49), KM12 (4.40), SW-620 (< 4.00)
CNS cancer	SF-268 (4.25), SF-295 (4.25), SF-539 (5.31), SNB-19 (4.41), SNB-75 (5.12), U251 (5.28)
Melanoma	LOX IMVI (5.23), MALME-3 M (4.37), M14 (4.44), SK-MEL-2 (4.93), SK-MEL-28 (4.32), SK-MEL-5 (4.79), UACC-257 (4.56), UACC-62 (5.07)
Ovarian cancer	IGROV1 (< 4.00), OVCAR-3 (4.66), OVCAR-4 (5.03), OVCAR-5 (4.43), OVCAR-8 (< 4.00), SK-OV-3 (4.63)
Renal cancer	786-0 (4.41), A498 (4.58), ACHN (4.47), CAKI-1 (4.26), RXF 393 (4.24), SN12C (4.69), TK-10 (4.61), UO-31 (4.46)
Prostate cancer	PC-3 (4.79), DU-145 (4.60)
Breast cancer	MCF7 (4.82), NCI/ADR-RES (4.12), MDA-MB-231/ATCC (5.01), HS 578 T (< 4.00), MDA-MB-435 (5.22), MDA-N (4.84), BT-549 (4.24), T-47D (< 4.00)

The candidate drug demonstrated inhibitory effects on the growth of a wide range of cancer cell lines generally

were sacrificed and tumors were evaluated for the degree of apoptosis and regression in addition to final volume.

Results obtained for the HCT-116 colon cancer: inhibition of tumor growth by the test substance NSC 710607 in the three schedules used, B, C, and D in Fig. 4, administered alone. The dose level of schedule B proved noticeably useful in both slackening tumor growth and increasing the life span of treated animals. MTD (maximum tolerated dose) was reached with 5 × 40 mg/kg (1/6 toxic deaths for C) in this human colon carcinoma xenograft assay. Moderate dose-dependent influence on BWC (body weight change) is seen.

The antitumor activity of NSC 710607 as a single treatment against human tumor xenografts is plainly visible in comparison with Saline/Tween® 80. NSC 710607 inhibited the growth of HCT-116 carcinoma xenografts, a dose of 20 mg/kg administered daily (100 mg as a single cycle) was the most effective. The T/C data show that NSC 710607 can be an effective agent in the chemotherapy of malignant tumors like HCT-116.

Data summarizing the in vivo MV-3 human melanoma xenografts on the compound NSC 710607 are shown in Table 5 and Fig. 5 ('training set' with at least some power of xenograft activity for human efficacy toward assessing the cancer models to appreciate in value in the second model). No influence on body weight and no considerable inhibition of tumor growth by the test substance are seen in all schedules used B-E (10, 20, 25, and 50 mg/kg treatment groups) with respect to the reference A. MTD with 2 × 50 mg/kg was apparently reached (1/6 toxic deaths for E). The trend of an increased death rate at higher doses is evident due to scheduling.

Clinically established platinum drugs

The therapeutic effect of Cisplatin (Fig. 6) is believed to result from the formation of covalent adducts with DNA. Highly reactive platinum complexes bind to nucleophilic groups in DNA (Zander et al. 2022; Wang 2010; Todd

Table 2 Cytostatic and cytotoxic effects of NSC 710608. Interactions take place at weaker AT-rich sequences in comparison with potent and tight, also less susceptible to mutation G–C pairs

4,6-Bis[4-(4,5-dihydro-4-methyl-1*H*-imidazol-2-yl)phenyl]-2-dimethylamino-1,3,5-triazine dihydrochloride	
Panel	Cell lines (cytotoxicity: pTGI > 4.00)
Leukemia	CCRF-CEM (5.46), HL-60(TB) (5.16), K-562 (5.10), MOLT-4 (5.27), RPMI-8226 (4.49)
Non-small cell lung cancer	A549/ATCC (4.88), EKVX (4.85), HOP-62 (5.32), HOP-92 (5.14), NCI-H23 (4.92), NCI-H322M (5.29), NCI-H460 (4.93), NCI-H522 (5.47)
Colon cancer	COLO 205 (5.62), HCC-2998 (5.41), HCT-116 (5.34), HCT-15 (4.47), HT29 (4.98), KM12 (5.25), SW-620 (5.09)
CNS cancer	SF-268 (5.13), SF-295 (4.84), SF-539 (5.66), SNB-19 (5.27), SNB-75 (5.49), U251 (5.62)
Melanoma	LOX IMVI (5.50), MALME-3 M (4.85), M14 (4.96), SK-MEL-2 (5.40), SK-MEL-28 (4.83), SK-MEL-5 (5.94), UACC-257 (5.35), UACC-62 (5.45)
Ovarian cancer	IGROV1 (4.80), OVCAR-3 (5.28), OVCAR-4 (5.45), OVCAR-5 (4.88), OVCAR-8 (5.03), SK-OV-3 (5.28)
Renal cancer	786–0 (5.07), A498 (5.04), ACHN (4.90), CAKI-1 (4.52), RXF 393 (4.99), SN12C (5.29), TK-10 (5.13), UO-31 (4.78)
Prostate cancer	PC-3 (5.33), DU-145 (5.31)
Breast cancer	MCF7 (5.31), NCI/ADR-RES (4.22), MDA-MB-231/ATCC (5.48), HS 578 T (4.83), MDA-MB-435 (5.52), MDA-N (5.32), BT-549 (4.85), T-47D (5.00)
Panel	Cell lines (cytotoxicity: $pLC_{50} > 4.00$)
Leukemia	CCRF-CEM (< 4.00), HL-60(TB) (4.35), K-562 (< 4.00), MOLT-4 (< 4.00), RPMI-8226 (< 4.00)
Non-small cell lung cancer	A549/ATCC (4.29), EKVX (4.31), HOP-62 (4.71), HOP-92 (4.37), NCI-H23 (4.28), NCI-H322M (4.71), NCI-H460 (4.40), NCI-H522 (5.13)
Colon cancer	COLO 205 (5.30), HCC-2998 (5.11), HCT-116 (4.80), HCT-15 (4.18), HT29 (4.47), KM12 (4.63), SW-620 (4.06)
CNS cancer	SF-268 (4.44), SF-295 (4.39), SF-539 (5.29), SNB-19 (4.71), SNB-75 (5.19), U251 (5.31)
Melanoma	LOX IMVI (5.17), MALME-3 M (4.40), M14 (4.47), SK-MEL-2 (5.10), SK-MEL-28 (4.39), SK-MEL-5 (4.47), UACC-257 (5.00), UACC-62 (5.16)
Ovarian cancer	IGROV1 (4.13), OVCAR-3 (4.75), OVCAR-4 (5.12), OVCAR-5 (4.44), OVCAR-8 (4.46), SK-OV-3 (4.74)
Renal cancer	786–0 (4.53), A498 (4.52), ACHN (4.45), CAKI-1 (4.26), RXF 393 (4.47), SN12C (4.77), TK-10 (4.59), UO-31 (4.35)
Prostate cancer	PC-3 (4.84), DU-145 (4.76)
Breast cancer	MCF7 (4.76), NCI/ADR-RES (< 4.00), MDA-MB-231/ATCC (5.13), HS 578 T (< 4.00), MDA-MB-435 (5.22), MDA-N (4.91), BT-549 (4.35), T-47D (4.14)

Comparable in vitro effects on 60 human tumor cell lines signify the DNA-binding mechanisms

Table 3 Relationship between the NCI in vitro parameters in log units and the in vivo hollow fiber assay, and its application to the drug discovery process

NSC code	pMG_MID	Range	Delta (Δ)	Δ_1 HCT-116	IP score	SC score	Cell kill
NSC 710607	5.73	1.67 (1.15)	0.72	0.53	18	6	Yes
NSC 710608	5.62	1.44 (0.76)	0.45	0.19	8	2	No

Tumor cell activities in such in vitro assays can predict in vivo chemotherapeutic responses

Table 4 Dose schedule, mortality, body weight change, and in vivo antitumor sensitivity of NSC 710607 against HCT-116 human colon carcinoma xenografts

Group	Nu/nu mice	Substance	Treatment (d)	Dose [mg/kg/inj.]	Toxic deaths (d)	BWC (%) d 9–16	Optimum *T/C* (%)
A	6	Saline/Tween® 80	9–13			16	
B	6	NSC 710607	9–13	20	0	− 9	61
C	6	NSC 710607	9–13	40	1 (14)	− 11	59
D	6	NSC 710607	9, 16	50	0	− 5	64

The in vivo drug experiments were performed to determine the sensitivity to various doses for comparison

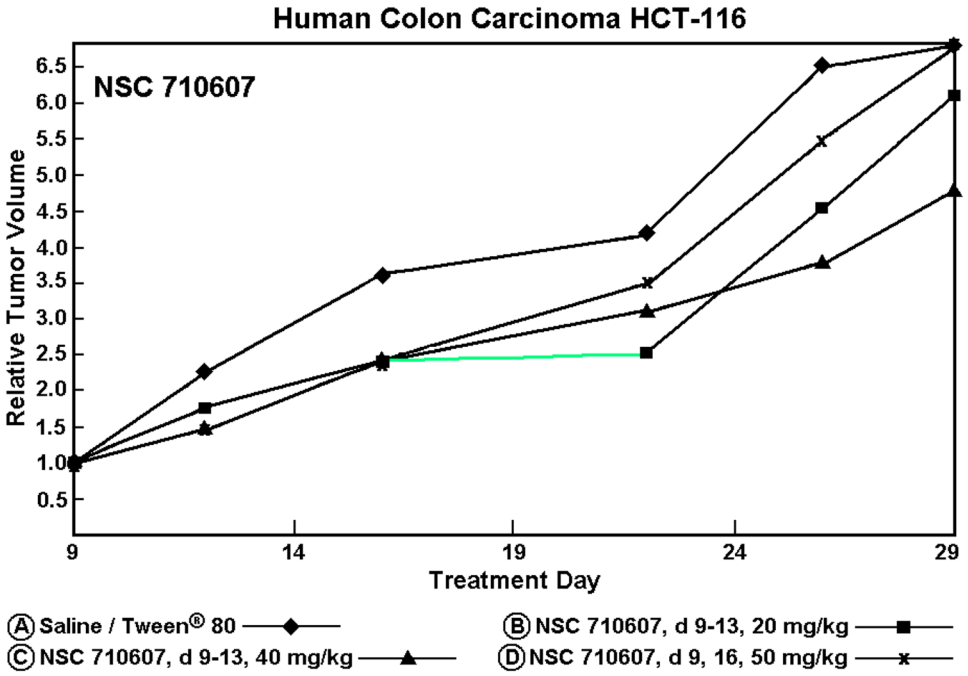

Fig. 4 Tumor growth inhibition of HCT-116 human colon carcinoma cells xenografted onto nude mice

Table 5 Dose schedule, mortality, body weight change, and in vivo antitumor sensitivity of NSC 710607 against MV-3 human melanoma xenografts

Group	Nu/nu mice	Substance	Treatment (d)	Dose [mg/kg/inj.]	Toxic deaths (d)	BWC (%) d 7–11	Optimum *T/C* (%)
A	6	Saline/Tween® 80	7–11			1	
B	6	NSC 710607	7–11	10	0	1	98
C	6	NSC 710607	7–11	20	0	1	93
D	6	NSC 710607	7, 14	25	0	5	157
E	6	NSC 710607	7, 14	50	1 (12)	− 1	122

Treatment resulted in marked increase in *T/C* (%) by comparison with the HCT-116 carcinoma xenografts

and Lippard 2009; Zhang et al. 2008; Jakupec et al. 2008; Guddneppanavar and Bierbach 2007; Torigoe et al. 2005). NSC 119875 (average GI_{50} over all cell lines 0.934 µM) is characterized by a DNA-binding mechanism dissimilar to that of NSC 710607, but their NCI sensitivity patterns are similar in appearance. Almost 40 platinum complexes are likely to produce biological activity complementary to that of Cisplatin (both NSC 241240 and NSC 266046 improve tumor bioavailability and toxicity profiles). All platinum drugs currently on the market require intravenous administration in contrast to an oral compound Satraplatin.

Clinically established Carboplatin is more stable and less toxic than Cisplatin and has been applied against ovarian carcinoma, lung, head, and neck cancers. Cisplatin is used in the treatment of metastatic ovarian or testicular cancers and advanced bladder cancer. Oxaliplatin has antitumor activity against colon carcinoma through its cytotoxic effects. Satraplatin is the most promising candidate with proven clinical efficacy and a more favorable toxicity profile (advanced prostate, lung, and ovarian) and clinical trial patients are able to take it at home. Mean graphs for medicinal drugs available from retail pharmacies: Carboplatin NSC 241240, Cisplatin NSC 119875, Oxaliplatin NSC 266046, and 5-fluorouracil NSC 27640 can be obtained from the NCI profiles.

Discussion

The NCI Biological Testing Branch of the Developmental Therapeutics Program has adopted a preliminary in vivo screening tool for assessing the potential anticancer activity of two triazine compounds recognized by the large-scale in vitro cell line screen. Many factors are considered in selecting these agents that receive additional evaluation as developmental candidates. Both NSC 710607 and NSC 710608 selected as leads were referred for prerequisite routine testing in the hollow fiber-based screen. The experimental data (IP + SC scores) show that the more flexible

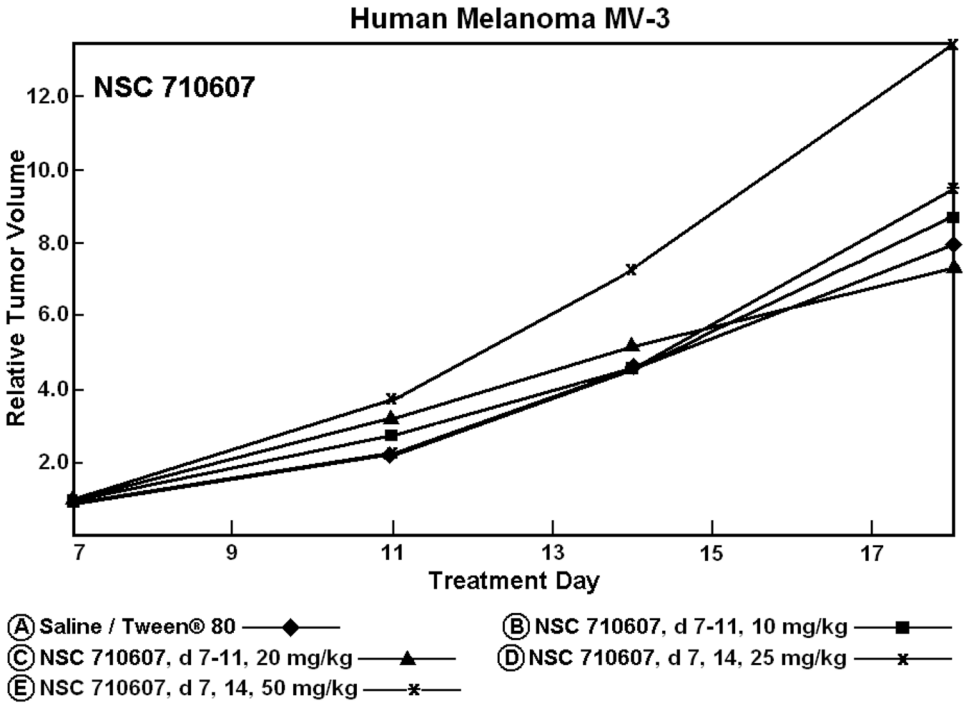

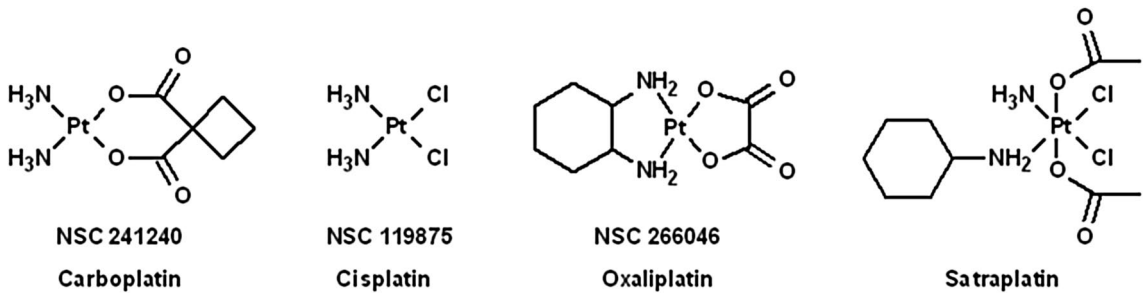

Fig. 5 Tumor growth inhibition of MV-3 human melanoma cells xenografted onto nude mice

Fig. 6 Platinum-containing chemotherapeutic agents. DNA–DNA and DNA–protein cross-links result in cell growth inhibition and apoptosis

molecule NSC 710607 can be an effective tool in further xenograft studies.

Mechanistic insight into such bisimidazoline compounds was previously published (Spychala et al. 1994). Thus, the paper does greatly increase our understanding of the potential action of these compounds. Triazine bisimidazolines bind to both DNA (minor groove interactions) and RNA (significant binding by intercalation) model sequences. The 2-dimethylaminotriazines give larger ΔT_m values than the unsubstituted triazines (interaction with poly dA·dT). The 4-methylimidazolines can exhibit significantly stronger binding to DNA and greater topoisomerase II inhibition by analogy to dicationic bistetrahydropyrimidines.

Efforts were put into description of minor groove binders by means of different anticancer parameters. The NCI-60 collective graphs served as a working model for explaining the targeting potential of drugs and to determine the underlying mechanism of tumor inhibition. A correlation between the tightness of all dose–response curves at GI_{50} level and size selectivity to DNA has been confirmed as a general phenomenon. The structural flexibility is responsible for the different selectivity to mutated centers of the two isomers NSC 710608 and NSC 710607. The latter was chosen for further experiments due to its apparent higher sensitivity.

The test substance NSC 710607 induced tumor apoptosis and promising inhibition of tumor growth in two nontoxic schedules used, but, the binding did not lead to a full recovery. From the potency parameters estimated—as judged by moderate body weight loss and mortality—it may be possible to predict the curative power (curative treatment) in the human tumor xenograft testing in nude mice. There is an overall correlation between the toxicity and the growth inhibition potency. The in vivo results offer a possibility

to narrow down the screening results in a dose- and time-dependent manner in colon cells.

This study demonstrates that NSC 710607 acts as general cytotoxic agents with predisposition to colorectal cancer in support of the DNA damage theory. Its comparative power of xenograft activity was assessed with MV-3. NSC 710607 decreased the T/C in colorectal cancer samples. One important fact must be taken under consideration that NSC 710607 was injected to mice only from days 9 to 13 (B scheduling) causing total cytostasis between the days 16 and 22. Considerable regression occurred after that time as a result of insufficient dosage. The in vitro data are of great significance for the in vivo effect. Treatment with NSC 710607 promises well for its utility in future. Efficacy of NSC 710607 on xenograft tumor in mice encourages investigating the possible ameliorative effects of NSC 710607 on more selective MOLT-4 cells.

An important difference exists between the DNA-binding mechanisms of NSC 710607 and platinum agents. While covalent interactions are an initial step in the mechanism of Cisplatin, which favor DNA structural perturbations resulting mainly from 1,2-intrastrand cross-links, DNA minor groove binders do not require this activation. The therapeutic effect of Cisplatin is believed to result from the formation of several covalent intra- and inter-strand charged adducts with DNA (primary target in cancer cells). These lesions provide the solid basis for Cisplatin-induced cytotoxicity. The multiplicity of DNA mechanisms and different mutated regions can influence the sensitivity. Cell death or survival in response to Cisplatin is dependent on the sensitivity patterns. The highest sensitivity is shown by colon, breast, and renal cancers.

Conclusion

In summary, the results (tumor cell activities in such as the NCI-60 in vitro assays) can predict drug sensitivity and extrapolate from one type of cancer to another, so they are likely to translate to rats and other research animal models or non-routine hollow fiber systems and specialized screening with alternate lines. NSC 710607 is likely to produce biological activity complementary to that of standard Cisplatin in a broad range of tumors. Important differences in structural perturbations exist between the DNA-binding mechanisms of NSC 710607 (noncovalent interactions) and Cisplatin (irreversible cross-links of bulky metal complexes). The noncovalent bonding interactions reflect the capacity to decrease cell proliferation. Findings confirmed that both NSC 710607 and NSC 710608 behave as DNA-binding antitumor antibiotics with great potential as general anticancer agents. NSC 710607 as a cure for cancer also has the HCT-116 superiority to an anticancer drug 5-fluorouracil. Treatment with NSC 710607 even without combination with other agents is full of promise.

Acknowledgements The author is thankful to Drs. V.L. Narayanan, E. Sausville (NIH, NCI, Bethesda, MD, USA), and Dr. M. Hollingshead (NCI, Frederick, MD, USA) for testing in an in vivo hollow fiber assay. He is forever in debt to Dr. I. Fichtner (Berlin, Germany) for the xenograft data provided within the framework of the EORTC/NCI worldwide activity.

Author contributions Broad conceptualization; methodology; formal analysis and investigation; writing—original draft preparation; writing—review and editing; supervision.

Funding The sole author has not disclosed any funding.

Data availability All data used to support the findings of this study are included within the article.

Declarations

Competing interests The single author declares no competing interests.

Conflict of interest The author has no relevant financial or non-financial interests to disclose.

Ethical approval All animal experiments were done according to the German Animal Protection Law.

Consent to publish Not applicable.

References

Boykin DW, Kumar A, Spychala J, Zhou M, Lombardy RJ, Wilson WD, Dykstra CC, Jones SK, Hall JE, Tidwell RR, Laughton C, Nunn CM, Neidle S (1995) Dicationic diarylfurans as anti-*Pneumocystis carinii* agents. J Med Chem 38:912–916. https://doi.org/10.1021/jm00006a009

Burden DA, Osheroff N (1998) Mechanism of action of eukaryotic topoisomerase II and drugs targeted to the enzyme. Biochim Biophys Acta 1400:139–154. https://doi.org/10.1016/s0167-4781(98)00132-8

Coleman LW, Rohr LR, Bronstein IB, Holden JA (2002) Human DNA topoisomerase I: an anticancer drug target present in human sarcomas. Hum Pathol 33:599–607. https://doi.org/10.1053/hupa.2002.124911

Dowling CM, Claffey J, Cuffe S, Fichtner I, Pampillon C, Sweeney NJ, Strohfeldt K, Watson RWG, Tacke M (2008) Antitumor activity of titanocene Y in xenografted PC3 tumors in mice. Lett Drug Des Disc 5:141–144. https://doi.org/10.2174/157018008783928463

Gu W, Li Y, Xia Y-Z, Yan T, Yang M-H, Kong L-Y (2022) Structural insight into the bulge-containing KRAS oncogene promoter G-quadruplex bound to berberine and coptisine. Nat Commun. https://doi.org/10.1038/s41467-022-33761-4

Guddneppanavar R, Bierbach U (2007) Adenine-N3 in the DNA minor groove—an emerging target for platinum containing anticancer pharmacophores. Anti-Cancer Agents Med Chem 7:125–138. https://doi.org/10.2174/187152007779313991

Hendry LB, Mahesh VB, Bransome ED Jr, Ewing DE (2007) Small molecule intercalation with double stranded DNA: implications for normal gene regulation and for predicting the biological

efficacy and genotoxicity of drugs and other chemicals. Mutat Res 623:53–71. https://doi.org/10.1016/j.mrfmmm.2007.03.009
Jakupec MA, Galanski MS, Arion VB, Hartinger CG, Keppler BK (2008) Antitumour metal compounds: more than theme and variations. Dalton Trans. https://doi.org/10.1039/B712656P
Kraus S, Arber N (2009) Inflammation and colorectal cancer. Curr Opinion Pharmacol 9:405–410. https://doi.org/10.1016/j.coph.2009.06.006
Li H-H, Aubrecht J, Fornace AJ Jr (2007) Toxicogenomics: overview and potential applications for the study of non-covalent DNA interacting chemicals. Mutat Res 623:98–108. https://doi.org/10.1016/j.mrfmmm.2007.03.013
Mastrangelo S, Attina G, Triarico S, Romano A, Maurizi P, Ruggiero A (2022) The DNA-topoisomerase inhibitors in cancer therapy. Biomed Pharmacol J 15:553–562. https://doi.org/10.13005/bpj/2396
McClendon AK, Osheroff N (2007) DNA topoisomerase II, genotoxicity, and cancer. Mutat Res 623:83–97. https://doi.org/10.1016/j.mrfmmm.2007.06.009
McConnaughie AW, Spychala J, Zhao M, Boykin D, Wilson WD (1994) Design and synthesis of RNA-specific groove-binding cations: implications for antiviral drug design. J Med Chem 37:1063–1069. https://doi.org/10.1021/jm00034a004
McIntyre RE, Buczacki SJA, Arends MJ, Adams David J (2015) Mouse models of colorectal cancer as preclinical models. BioEssays 37:909–920. https://doi.org/10.1002/bies.201500032
Nelson SM, Ferguson LR, Denny WA (2007) Non-covalent ligand/DNA interactions: minor groove binding agents. Mutat Res 623:24–40. https://doi.org/10.1016/j.mrfmmm.2007.03.012
Ogbonna EN, Paul A, Ross Terrell J, Fang Z, Chen C, Poon GMK, Boykin DW, Wilson WD (2022) Drug design and DNA structural research inspired by the Neidle laboratory: DNA minor groove binding and transcription factor inhibition by thiophene diamidines. Bioorg Med Chem. https://doi.org/10.1016/j.bmc.2022.116861
Plowman J, Dykes DJ, Hollingshead M, Simpson-Herren L, Alley MC (1997) Preclinical screening, clinical trials, and approval. In: Teicher B (ed) Anticancer drug development guide. Humana Press, Totowa, pp 101–125
Shoemaker RH (2006) The NCI60 human tumour cell line anticancer drug screen. Nat Rev Cancer 6:813–823. https://doi.org/10.1038/nrc1951
Spychala J (1999) A general synthesis of diaryl cyclic diamidines. Tetrahedron Lett 40:2841–2844. https://doi.org/10.1016/S0040-4039(99)00307-X
Spychala J (2006) A convenient way to methylated 2-imidazolines. Syntheses of fluorene and triazine cyclic diamidines. Monatsh Chem 137:1203–1210. https://doi.org/10.1007/s00706-006-0516-y
Spychala J (2008) The usefulness of cyclic diamidines with different core-substituents as antitumor agents. Bioorg Chem 36:183–189. https://doi.org/10.1016/j.bioorg.2008.05.002
Spychala J (2009) Selective cytostatic and cytotoxic anticancer effects of bisfunctional agents: a strategy for the design of DNA binding agents. Cancer Lett 281:203–212. https://doi.org/10.1016/j.canlet.2009.02.026
Spychala J, Boykin DW, Wilson WD, Zhao M, Tidwell RR, Dykstra CC, Hall JE, Jones SK, Schinazi RF (1994) Synthesis of dicationic diaryltriazines nucleic acid binding agents. Eur J Med Chem 29:363–367. https://doi.org/10.1016/0223-5234(94)90061-2
Syriopoulou E, Morris E, Finan PJ, Lambert PC, Rutherford MJ (2019) Understanding the impact of socioeconomic differences in colorectal cancer survival: potential gain in life-years. Br J Cancer 120:1052–1058. https://doi.org/10.1038/s41416-019-0455-0
Todd RC, Lippard SJ (2009) Inhibition of transcription by platinum antitumor compounds. Metallomics 1:280–291. https://doi.org/10.1039/b907567d
Torigoe T, Izumi H, Ishiguchi H, Yoshida Y, Tanabe M, Yoshida T, Igarashi T, Niina I, Wakasugi T, Imaizumi T, Momii Y, Kuwano M, Kohno K (2005) Cisplatin resistance and transcription factors. Curr Med Chem Anti-Cancer Agents 5:15–27. https://doi.org/10.2174/1568011053352587
Torkamani A, Verkhivker G, Schork NJ (2009) Cancer driver mutations in protein kinase genes. Cancer Lett 281:117–127. https://doi.org/10.1016/j.canlet.2008.11.008
Van Cutsem E, Lenz H-J, Kohne C-H, Heinemann V, Tejpar S, Melezinek I, Beier F, Stroh C, Rougier P, van Krieken JH, Ciardiello F (2015) Fluorouracil, leucovorin, and irinotecan plus cetuximab treatment and RAS mutations in colorectal cancer. J Clin Oncol 33:692–700. https://doi.org/10.1200/JCO.2014.59.4812
Wang X (2010) Fresh platinum complexes with promising antitumor activity. Anti-Cancer Agents Med Chem 10:396–411. https://doi.org/10.2174/1871520611009050396
Wemmer DE, Dervan PB (1997) Targeting the minor groove of DNA. Curr Opinion Struct Biol 7:355–361. https://doi.org/10.1016/S0959-440X(97)80051-6
Xie B, Wang Y, Wang D, Xue X, Nie Y (2022) Synthesis, characterization and anticancer efficacy studies of iridium (III) polypyridyl complexes against colon cancer HCT116 cells. Molecules 27:5434. https://doi.org/10.3390/molecules27175434
Zander T, Xue J, Markson G, Dahm F, Renner C (2022) Satraplatin demonstrates high cytotoxic activity against genetically defined lymphoid malignancies. Anticancer Res 42:1821–1832. https://doi.org/10.21873/anticanres.15658
Zhang J, Gong Y, Zheng X, Yang M, Cui J (2008) Synthesis, cytotoxicity and DNA binding levels of tri-functional mononuclear platinum(II) complexes. Eur J Med Chem 43:441–447. https://doi.org/10.1016/j.ejmech.2007.04.015
Zhang B, Lin J, Perculija V, Li Y, Lu Q, Chen J, Ouyang S (2022) Structural insights into target DNA recognition and cleavage by the CRISPR-Cas12c1 system. Nucleic Acids Res. https://doi.org/10.1093/nar/gkac987